Chapter 2

BETATRON TUNE SHIFTS

2.1 STATIC TRANSVERSE FORCES

The vertical motion of a beam particle inside a beam obeys the equation of motion

$$\frac{dp_y}{dt} = F_{\rm ext}(y) + F_{\rm beam}(y, \bar{y}) \ , \tag{2.1}$$

where $p_y = \gamma m dy/dt$ is the vertical momentum of the particle and m its rest mass. We are studying small amount of vertical motion and γ can therefore taken out of the derivative. Here, $F_{\rm ext}(y)$ is the force due to the magnets outside the vacuum chamber and gives rise to betatron oscillations, while $F_{\rm beam}(y, \bar{y})$ is the force on the particle at y and the beam vertical center at $\bar{y}$ coming from the electromagnetic fields of the beam. For example, with quadrupole focusing,

$$F_{\rm ext}(y) = \frac{B'_y}{B\rho}\, y \qquad \text{with} \qquad B'_y = \frac{dB_y}{dx} \ , \tag{2.2}$$

where dB_y/dx is the gradient of the quadrupole magnetic flux density and $B\rho$ the rigidity of the beam. If we consider this focusing to be uniform along the accelerator ring while keeping y fixed, we obtain

$$\langle F_{\rm ext}(y) \rangle \longrightarrow -(\nu_0^V \omega_0)^2 y \ , \tag{2.3}$$

where ν_0^V is the number of vertical oscillations the particle makes in a turn or what we usually called the *bare* vertical betatron tune, while $\omega_0/(2\pi)$ is the revolution frequency.

Notice that the average of the external force is proportional to the impulse in one accelerator turn. Now the transverse equation of motion becomes

$$\frac{d^2y}{ds^2} + \frac{(\nu_0^V)^2}{R^2} = \frac{\langle F_{\rm beam}(y,\bar{y})\rangle}{\gamma m v^2} \tag{2.4}$$

where R is the average radius of the ring and m the rest mass of the beam particles. In above, the rigid-bunch and impulse approximations have been applied to the $F_{\rm beam}$, and we have replaced d/dt by vd/ds with v the velocity of the beam and s the distance measured along the longitudinal path in the ring. In this chapter, we are going to study the steady-state effects of the transverse wake potential on the beam. Therefore, there is no explicit time dependency in $\langle F_{\rm beam}\rangle$. As will be shown below, the steady-state effects of the wake potential contribute to betatron tune shifts, while the time-dependent effects may excite instabilities.

Since we are interested only in small amount of motion in the vertical direction, we can Taylor expand the beam force to obtain

$$\frac{d^2y}{ds^2} + \frac{(\nu_0^V)^2}{R^2}y = \frac{1}{\gamma m v^2}\left(\left.\frac{\partial\langle F_{\rm beam}\rangle}{\partial y}\right|_{\bar{y}=0} y + \left.\frac{\partial\langle F_{\rm beam}\rangle}{\partial \bar{y}}\right|_{y=0}\bar{y}\right) , \tag{2.5}$$

The first term on the right side is proportional to the vertical displacement of the witness particle; it therefore constitute a shift of the vertical betatron tune ν_0^V to become $\nu_{\rm incoh}^V$. When the shift is small, we write $\left(\nu_{\rm incoh}^V\right)^2 = \left(\nu_0^V\right)^2 + 2\nu_0^V\Delta\nu_{\rm incoh}^V$ with

$$\Delta\nu_{\rm incoh}^V = -\frac{R^2}{2\nu_{0y}\gamma m v^2}\left.\frac{\partial\langle F_{\rm beam}\rangle}{\partial y}\right|_{\bar{y}=0} . \tag{2.6}$$

Since this shift affects an individual beam particle, it is called the *incoherent tune shift*. Thus, the incoherent tune shift can be computed by setting $\bar{y} = 0$ or without any displacement of the center of the whole beam.

Now coming back to Eq. (2.5), the transverse equation of motion. We can write one such equation for each beam particle. We perform an average by adding up these equations and dividing by the total number of beam particles. The result is

$$\frac{d^2\bar{y}}{ds^2} + \frac{(\nu_0^V)^2}{R^2}\bar{y} = \frac{1}{\gamma m v^2}\left(\left.\frac{\partial\langle F_{\rm beam}\rangle}{\partial y}\right|_{\bar{y}=0}\bar{y} + \left.\frac{\partial\langle F_{\rm beam}\rangle}{\partial \bar{y}}\right|_{y=0}\bar{y}\right) , \tag{2.7}$$

This equation describes now the vertical motion of the center of the beam, or the *coherent motion* of the beam, which is just a simple harmonic motion. The vertical betatron tune

of the center of the beam, or the *coherent* vertical betatron tune of the beam, is now $\nu^V_{\rm coh} = \nu^V_0 + \Delta\nu^V_{\rm coh}$. When the perturbation is small, the coherent tune shift becomes

$$\Delta\nu^V_{\rm coh} = -\frac{R^2}{2\nu^V_0\gamma m v^2}\left(\left.\frac{\partial\langle F_{\rm beam}\rangle}{\partial y}\right|_{\bar y=0} + \left.\frac{\partial\langle F_{\rm beam}\rangle}{\partial \bar y}\right|_{y=0}\right) . \tag{2.8}$$

Let us assume here that the vacuum chamber is completely smooth and infinitely conducting. Then the force on a beam particle from the beam comes from only two sources: (1) electromagnetic interaction of the beam particle with all other beam particles in the beam, which we call *self-force*, (2) reflection of electromagnetic fields from the walls of the vacuum chamber, which we call *image forces*.

2.2 ELECTRIC IMAGE FORCES

The image forces certainly depends on the geometry of the vacuum chamber. Let us consider the simple case when the vacuum chamber consists of two infinite horizontal plates at location $y = \pm h$ as illustrated in Fig. 2.1. The beam of say positive charges is displaced by $\bar y_1$ vertically and the witness particle is at y_1. We wish to consider the electric force on the witness particle coming from reflection by the top and bottom walls of the vacuum chamber. In order that the horizontal electric field at the top and bottom walls vanishes, there must be an image of the beam with negative charges at position $y = 2h - \bar y_1$ or at a distance $2h - \bar y_1 - y_1$ from the witness particle. This image will have another image of positive charges from the bottom wall at $y = -(4h - \bar y_1)$ or $4h - \bar y_1 + y$ from the witness particle. This secondary image will have a third image from the top wall, etc.

Similarly, the beam will have an image of negative charges from the bottom wall at $y = -(2h + \bar y_1)$ or $2h + \bar y_1 + y_1$ from the witness particle. This image will form another image through the top wall with positive charges at $y = 4h + \bar y_1$ or $4h + \bar y_1 - y_1$ from the witness particle, etc. Summing up, the vertical electric field acting on the witness particle is

$$\begin{aligned} E_y = \frac{e\lambda}{2\pi\epsilon_0}\Bigg[&\frac{1}{2h-\bar y_1-y_1} - \frac{1}{2h+\bar y_1+y_1} + \frac{1}{6h-\bar y_1-y_1} - \frac{1}{6h+\bar y_1+y_1} + \cdots \\ &-\frac{1}{4h+\bar y_1-y_1} + \frac{1}{4h-\bar y_1+y_1} - \frac{1}{8h-\bar y_1-y_1} + \frac{1}{8h+\bar y_1+y_1} + \cdots\Bigg] , \end{aligned} \tag{2.9}$$

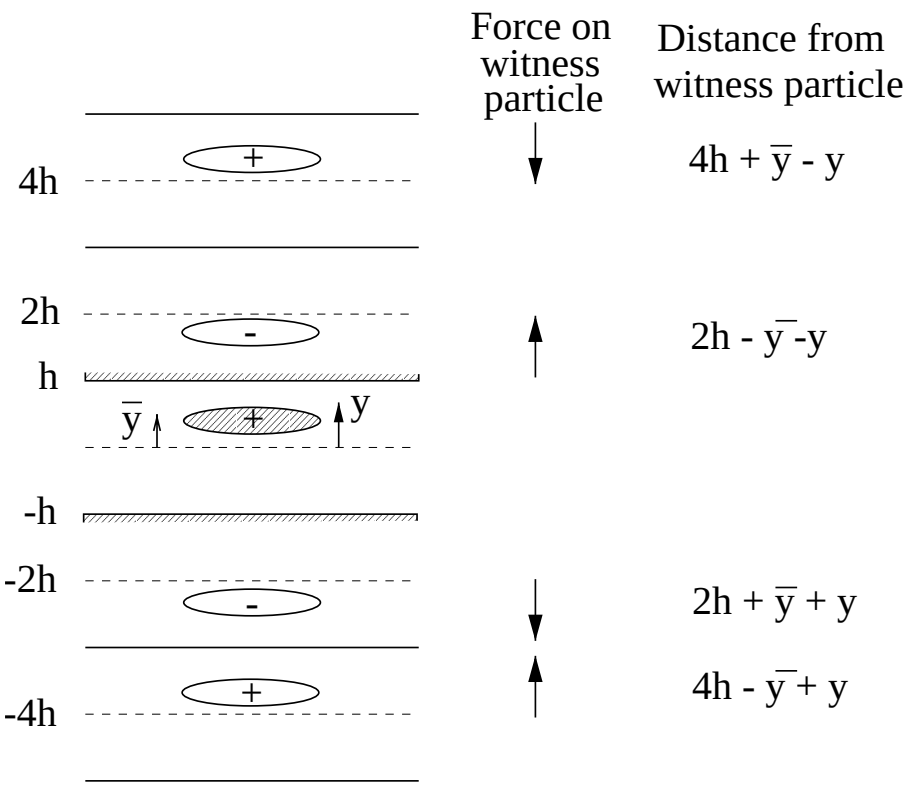

Figure 2.1: Illustration showing the electric forces from the images of a beam, off centered vertically by $\bar{y}$, acting on a witness particle at location y inside the beam between two infinite horizontal conducting parallel plates separated vertically by distance $2h$.

where λ is the linear particle density per unit length along the ring. Every two adjacent terms are grouped together giving

$$E_y = \frac{e\lambda}{2\pi\epsilon_0}\Bigg[+\frac{2(\bar{y}_1+y_1)}{(2h)^2-(\bar{y}_1+y_1)^2} + \frac{2(\bar{y}_1+y_1)}{(6h)^2-(\bar{y}_1+y_1)^2} + \cdots + \frac{2(\bar{y}_1-y_1)}{(4h)^2-(\bar{y}_1-y_1)^2} + \frac{2(\bar{y}_1-y_1)}{(8h)^2-(\bar{y}_1-y_1)^2} + \cdots \Bigg] . \tag{2.10}$$

Since we consider only small vertical motion, only terms linear in $\bar{y}_1+y_1$ and $\bar{y}_1-y_1$ are kept leading to

$$\begin{aligned} E_y &= \frac{e\lambda}{\pi\epsilon_0 h^2}\left[(\bar{y}_1+y_1)\left(\frac{1}{2^2}+\frac{1}{6^2}+\frac{1}{10^2}+\cdots\right)+(\bar{y}_1-y_1)\left(\frac{1}{4^2}+\frac{1}{8^2}+\frac{1}{12^2}+\cdots\right)\right] \\ &= \frac{e\lambda}{\pi\epsilon_0 h^2}\left[(\bar{y}_1+y_1)\frac{\pi^2}{32}+(\bar{y}_1-y_1)\frac{\pi^2}{96}\right] . \end{aligned} \tag{2.11}$$

In the literature, there is a standard way to write these image contributions following the work of Laslett [1, 2]:

$$E_y = \frac{e\lambda}{\pi\epsilon_0}\frac{\epsilon_1^V}{h^2}y_1 \qquad \text{and} \qquad \frac{e\lambda}{\pi\epsilon_0}\frac{\xi_1^V}{h^2}\bar{y}_1 \ , \tag{2.12}$$

where ϵ_1^V and ξ_1^V are called, respectively, the incoherent and coherent electric image coefficients. For the situation of two parallel plates, we have $\epsilon_1^V = \pi^2/48$ and $\xi_1^V = \pi^2/16$. Attention should be paid that in deriving the coherent image coefficient, y_1 has been replaced by $\bar{y}_1$ in Eq. (2.9) or (2.10) or (2.11). According to Eqs. (2.6) and (2.8), the coherent and incoherent vertical tune shifts due to electric images are:

$$\Delta\nu^V_{\text{incoh}} = -\frac{Nr_0R}{\pi\gamma\beta^2\nu_0^V}\frac{\epsilon_1^V}{h^2} \qquad \text{and} \qquad \Delta\nu^V_{\text{coh}} = -\frac{Nr_0R}{\pi\gamma\beta^2\nu_0^V}\frac{\xi_1^V}{h^2} \ , \tag{2.13}$$

where we have replaced the linear particle density by $\lambda = N/(2\pi R)$ with N being the total number of particles in the beam, and introduced the classical radius of the particle $r_0 = e^2/(4\pi\epsilon_0 mc^2)$.

2.3 MAGNETIC IMAGE FORCES

Unlike the electric field that cannot penetrate the metallic vacuum chamber at any frequency, the effect of the magnetic field is more complex. The magnet field has an ac component and a dc component. The ac component has its component parallel to the wall of the vacuum chamber converted into eddy current. In other words, the ac magnetic field *cannot* penetrate the wall of the vacuum chamber. There the boundary condition is $B_\perp = 0$. To accomplish this, the first image from a boundary wall give image currents that flow in the opposite direction to that the beam. The total force from these magnetic images acting on the witness charge current at position y_1 is illustrated in Fig. 2.2 and is expressed as

$$\begin{aligned}\frac{F_y^{\text{mag}}}{e} = -\frac{e\mu_0\lambda v^2}{2\pi}\Bigg[&\frac{1}{2h-\bar{y}_1-y_1} - \frac{1}{2h+\bar{y}_1+y_1} + \frac{1}{6h-\bar{y}_1-y_1} - \frac{1}{6h+\bar{y}_1+y_1} + \cdots \\ &- \frac{1}{4h+\bar{y}_1-y_1} + \frac{1}{4h-\bar{y}_1+y_1} - \frac{1}{8h-\bar{y}_1-y_1} + \frac{1}{8h+\bar{y}_1+y_1} + \cdots \Bigg] .\end{aligned} \tag{2.14}$$

There is the factor v^2 outside the square brackets on the right side. One v comes from the source beam current and the other v comes from the Lorentz force. It is interesting

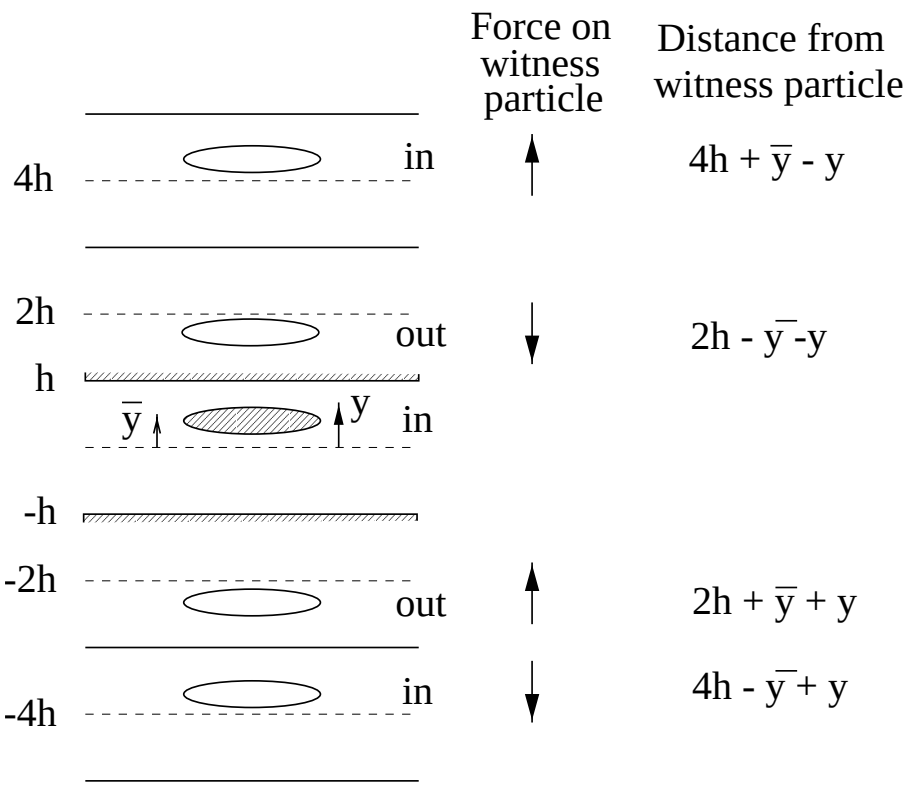

Figure 2.2: Illustration showing the magnetic forces from the images of a beam, off centered vertically by $\bar{y}$, acting on a witness current at location y inside the beam between two infinite horizontal conducting parallel plates separated vertically by distance $2h$. The normal components of the non-penetrating magnetic fields vanish at the plates. The beam or image currents flowing into or out of the paper are labeled "in" or "out".

to see that this factor is equal to $-e\lambda\beta^2/(2\pi\epsilon_0)$. Thus, the force due to the ac magnetic images are just a factor $-\beta^2$ different from the force due to the electric images. This leads to

$$\frac{F_y^{\rm mag}}{e} = -\frac{e\lambda\beta^2}{2\pi\epsilon_0 h^2}\left[(\bar{y}_1+y_1)\frac{\pi^2}{32}+(\bar{y}_1-y_1)\frac{\pi^2}{96}\right] . \tag{2.15}$$

Following Eq. (2.13), we write the tune shifts due to ac magnetic images as

$$\Delta\nu^V_{\rm incoh} = \frac{Nr_0R}{\pi\gamma\nu_0^V}\frac{\epsilon_1^V}{h^2} \qquad \text{and} \qquad \Delta\nu^V_{\rm coh} = \frac{Nr_0R}{\pi\gamma\nu_0^V}\frac{\xi_1^V}{h^2} . \tag{2.16}$$

There is always a dc part of the magnetic field that can penetrate the wall of the beam pipe and lands on the pole faces of the magnet as if the vacuum chamber is not there.

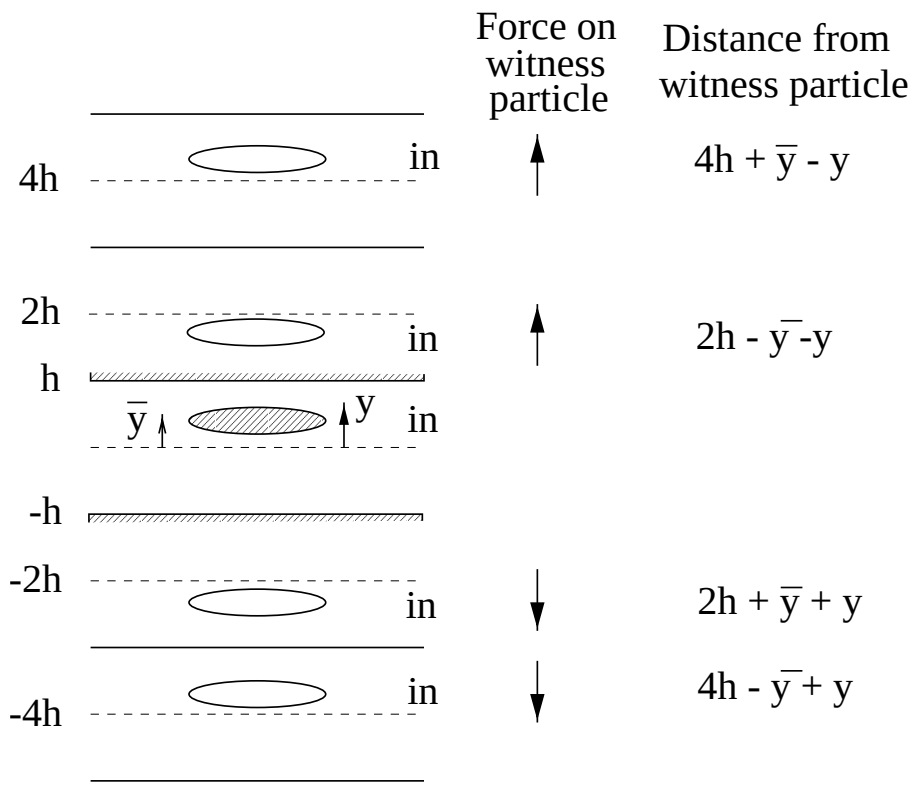

Figure 2.3: Illustration showing the magnetic forces from the images of a beam, off centered vertically by $\bar{y}$, acting on a witness current at location y inside the beam between two infinite horizontal conducting parallel plates separated vertically by distance $2h$. The parallel components of the penetrating magnetic fields vanish at the plates. Here, the beam and all image currents flow into the paper.

The boundary condition on the magnet pole faces is now $B_\perp$ continuous and $B_\parallel = 0$. In order to accommodate this, all the image currents must flow in exactly the same direction of the source beam, as is illustrated in Fig. 2.3. The force on the witness particle is now

$$\frac{F_y^{\rm mag}}{e} = \frac{e\mu_0\lambda v^2}{2\pi}\left[\frac{1}{2g-\bar{y}_1-y_1} - \frac{1}{2g+\bar{y}_1+y_1} + \frac{1}{6g-\bar{y}_1-y_1} - \frac{1}{6g+\bar{y}_1+y_1} + \cdots \right.$$
$$\left. + \frac{1}{4g+\bar{y}_1-y_1} + \frac{1}{4g-\bar{y}_1+y_1} + \frac{1}{8g-\bar{y}_1-y_1} - \frac{1}{8g+\bar{y}_1+y_1} + \cdots\right], \quad (2.17)$$

where the magnetic pole faces are at $y = \pm g$ or the magnets have a vertical gap $2g$ between the poles faces. It is important to note the slight difference between Eqs. (2.14)

and (2.17). Here we obtain

$$\frac{F_y^{\rm mag}}{e} = +\frac{e\lambda\beta^2}{2\pi\epsilon_0 g^2}\left[(\bar{y}_1+y_1)\frac{\pi^2}{32} - (\bar{y}_1-y_1)\frac{\pi^2}{96}\right] . \tag{2.18}$$

as compared to Eq. (2.15). Following Laslett, we write the tune shifts due to ac magnetic images as

$$\Delta\nu^V_{\rm incoh} = -\frac{Nr_0R}{\pi\gamma\nu_0^V}\frac{\epsilon_2^V}{g^2} \qquad \text{and} \qquad \Delta\nu^V_{\rm coh} = -\frac{Nr_0R}{\pi\gamma\nu_0^V}\frac{\xi_2^V}{g^2} , \tag{2.19}$$

where ϵ_2^V and ξ_2^V are called, respectively, the vertical incoherent and coherent dc magnetic image coefficients. For the special case of two parallel plates, we have here $\epsilon_2^V = \pi^2/24$ and $\xi_2^V = \pi^2/16$.

It is important to remind ourselves that by penetrating or non-penetrating magnetic fields, we refer the the magnetic fields exerted on the witness and coming from the *center* of the beam or the *coherent motion* of the beam and all its images.

There is also a set of horizontal image coefficients: ϵ_1^H, ϵ_2^H, ξ_1^H, and ξ_2^H. Because the point of observation is source-free, $\vec{\nabla}\cdot\vec{E} = 0$ and $\vec{\nabla}\cdot\vec{B} = 0$, we always have

$$\epsilon_1^H = -\epsilon_1^V \qquad \text{and} \qquad \epsilon_2^H = -\epsilon_2^V . \tag{2.20}$$

On the other hand, there is no definite relationship between the horizontal and vertical coherent electric image coefficients. In the special case of two parallel plates, it is obvious that $\xi_1^H = 0$ and $\xi_2^H = 0$, which is the result of translational invariance.

It is important to point out that electric and magnetic image coefficients are always defined with reference to the *half vertical* vacuum chamber h or the square of the *half vertical* magnetic pole gap g, independent of whether we are talking about the vertical or horizontal tune shifts. For the example of a rectangular beam pipe of half height h and half width w, only h^2 will enter into the denominators but never w^2, such as in Eqs. (2.13), (2.16), or (2.19). In the same way, for an elliptical beam pipe of vertical radius b and horizontal radius a, the image coefficients will be defined with reference to $h = b$ but not a. It is because of such a dedicated reference that the relations in Eq. (2.20) hold.

2.4 SELF FORCE

The interaction of a beam particle with other beam particles in the beam depends on the transverse distribution of the beam. Let us first consider a uniformly distributed

coasting beam of radius a. The witness particle at $y = y_1 \leq a$ sees, in the y direction, an electric force

$$F_y^{\text{elect}} = \frac{e^2\lambda}{2\pi\epsilon_0 a^2}\left(y_1 - \bar{y}_1\right) , \tag{2.21}$$

and a magnetic force

$$F_y^{\text{mag}} = -\frac{e^2\mu_0\lambda v^2}{2\pi a^2}\left(y_1 - \bar{y}_1\right) = -\frac{e^2\lambda\beta^2}{2\pi\epsilon_0 a^2}\left(y_1 - \bar{y}_1\right) , \tag{2.22}$$

or a total force of

$$F_y = \frac{e^2\lambda}{2\pi\epsilon_0\gamma^2 a^2}\left(y_1 - \bar{y}_1\right) . \tag{2.23}$$

where $\bar{y}_1$ is vertical position of the center of the beam. This self force is a space-charge force. According to Eq. (2.6), this self force lead to a space-charge tune shift of

$$\Delta\nu^{V,H}_{\text{spch incoh}} = -\frac{Nr_0R}{2\pi\gamma^3\beta^2a^2\nu_0^{V,H}} . \tag{2.24}$$

It is clear from Eq. (2.23) that the coherent space-charge tune shifts in both transverse directions are zero. This is understandable, because the center of the beam does not see its own space-charge force. We can also define self-field or space-charge coefficients in the vertical and horizontal directions, $\epsilon^{V,H}_{\text{spch}} = \frac{1}{2}$, such that

$$\Delta\nu^{V,H}_{\text{spch incoh}} = -\frac{Nr_0R}{\pi\gamma^3\beta^2\nu_0^{V,H}}\frac{\epsilon^{V,H}_{\text{spch}}}{a^2} . \tag{2.25}$$

The space-charge coefficients take care of the transverse shape of the beam and how the beam particles are distributed.

We can also express the incoherent space charge tune shift in term of the normalized emittance of the beam

$$\epsilon_N^{V,H} = \gamma\beta\frac{a^2}{\langle\beta_{V,H}\rangle} , \tag{2.26}$$

where $\langle\beta_{V,H}\rangle$ is the average vertical/horizontal betatron function of the ring, which is roughly equal to $R/\nu_0^{V,H}$. Then, we have

$$\Delta\nu^{V,H}_{\text{spch incoh}} = -\frac{Nr_0}{2\pi\gamma^2\beta\epsilon_N^{V,H}B} . \tag{2.27}$$

In the above, we have also introduced the single-bucket bunching factor B to take care of the fact the the beam may be longitudinally bunched. The single-bucket bunching factor is defined as

$$B = \frac{I_{\text{av}}}{I_{\text{pk}}} , \tag{2.28}$$

where $I_{\rm av}$ and $I_{\rm pk}$ are, respectively, the current of a bunch averaged over a *single* rf bucket and its peak current, or the average current to the peak current assuming that all the buckets are filled.

We can also consider a transverse bi-Gaussian distribution of the beam,

$$f(x,y) = \frac{N}{2\pi\sigma^2} e^{-(x^2+y^2)/(2\sigma^2)} \ , \tag{2.29}$$

where σ is the rms transverse spread of the beam. A particle at $y = y_1$ will see an electric force in the y direction,

$$F_y^{\rm elect} = \frac{e^2}{2\pi\epsilon_0 y_1}\frac{N}{\sigma^2}\int_0^{y_1} e^{-r^2/(2\sigma^2)} r dr = \frac{e^2 N}{2\pi\epsilon_0 y_1}\left[1 - e^{-y_1^2/(2\sigma^2)}\right] \ . \tag{2.30}$$

For small offset, $y_1 \ll \sigma$, we have

$$F_y^{\rm elect} = \frac{e^2 N}{4\pi\epsilon_0\sigma^2} y_1 \ . \tag{2.31}$$

The magnetic force is the same multiplied by $-\beta^2$. The incoherent space-charge tune shift is therefore

$$\Delta\nu_{\rm spch\ incoh}^{V,H} = -\frac{N r_0 R}{4\pi\gamma^3\beta^2\sigma^2\nu_0^{V,H}} \ . \tag{2.32}$$

Here, we can define the 95% normalized transverse emittance $\epsilon_{N95}^{V,H}$ of the beam which encloses 95% of the beam particles. This corresponds to a radius r_{95} given by

$$\frac{1}{2\pi\sigma^2}\int_0^{r_{95}} e^{-r^2/(2\sigma^2)} 2\pi r dr = 95\% \ , \tag{2.33}$$

which gives $r_{95} \approx \sqrt{6}\sigma$. Thus

$$\epsilon_{N95}^{V.H} = \gamma\beta\frac{r_{95}^2}{\langle\beta_{V,H}\rangle} = \gamma\beta\frac{6\sigma^2}{\langle\beta_{V,H}\rangle} \ . \tag{2.34}$$

The space-charge tune shift becomes

$$\Delta\nu_{\rm spch\ incoh}^{V,H} = -\frac{3N r_0}{2\pi\gamma^2\beta\epsilon_{N95}^{V,H} B} \ . \tag{2.35}$$

This tune shift is three times as large as the tune shift for a uniform distribution in Eq. (2.27). This is because the linear particle density at the bunch center is much larger if the distribution is uniform.

As is seen in Eq. (2.30), the transverse space-charge force is not linear. For the bi-Gaussian distribution, for example, the incoherent space-charge tune shift is largest when the witness particle is at the center of the beam and decreases as transverse offset increases. For this reason, the incoherent space-charge tune shift is in fact a tune spread, which may encompass a number of resonances in the ν^V-ν^H tune space. Those particles that fall inside a resonant stop band will be lost. The beam intensity in low-energy synchrotrons is usually limited by this space-charge tune spread. As a rule of thumb, the incoherent space-charge tune shift has to be kept under ~ 0.4. At the same time, the widths of important stop bands have been minimized by corrections made to the ring lattice.

2.5 COASTING BEAMS

For a coasting beam the ac magnetic field can only come from betatron oscillation of the beam and is non-penetrating. The incoherent tune shift, according to Eq. (2.6), arrives from the betatron oscillation of a beam particle inside a beam that is not oscillating. The beam particle therefore sees only dc or penetrating magnetic field from the bunch and all its images. Gathering all the contributions, the incoherent tune shifts for a coasting beam are

$$\Delta\nu^{V,H}_{\rm incoh} = -\frac{Nr_0R}{\pi\gamma\beta^2\nu_0^{V,H}}\left[\frac{\epsilon_1^{V,H}}{h^2} + \mathcal{F}\beta^2\frac{\epsilon_2^{V,H}}{g^2} + (1-\beta^2)\frac{\epsilon^{V,H}_{\rm spch}}{a_V^2}\right], \tag{2.36}$$

$\uparrow$ electric image in vacuum chamber; $\uparrow$ magnetic image in magnet poles; $\uparrow$ self-field, $(1-\beta^2)$ gives balance between for $\vec{E}$ and $\vec{H}$

where in the self-field term, a_V is the vertical radius of the beam and $\epsilon^{V,H}_{\rm spch} = \frac{1}{2}$ if the beam is circular. In the term involving magnetic image in the magnet poles, $\mathcal{F}$ is the fraction of the beam pipe enclosed by magnets.

For coherent motion with only dc magnetic field, which is penetrating, from the bunch and its images, we must use the magnetic penetrating image coefficients $\xi_2^{V,H}$. The coherent tune shift with penetrating magnetic field is

$$\Delta\nu^{V,H}_{\rm coh} = -\frac{Nr_0R}{\pi\gamma\beta^2\nu_0^{V,H}}\left[\frac{\xi_1^{V,H}}{h^2} + \mathcal{F}\beta^2\frac{\xi_2^{V,H}}{g^2}\right]. \tag{2.37}$$

$\uparrow$ electric image in vacuum chamber; $\uparrow$ magnetic image in magnet poles

For coherent motion with non-penetrating fields, the tune shift is

$$\Delta\nu_{\rm coh}^{V,H} = -\frac{Nr_0R}{\pi\gamma\beta^2\nu_0^{V,H}}\left[\frac{\xi_1^{V,H}}{h^2} + \mathcal{F}\beta^2\frac{\epsilon_2^{V,H}}{g^2} - \beta^2\frac{\xi_1^{V,H}-\epsilon_1^{V,H}}{h^2}\right] . \tag{2.38}$$

$$\begin{array}{ccc} \uparrow & \uparrow & \uparrow \\ \text{electric image} & \text{magnetic image} & \text{ac magnetic image} \\ \text{in vacuum chamber} & \text{in magnet poles} & \text{in vacuum chamber} \end{array}$$

To understand this expression, let us, for simplicity, discuss just the vertical force. Recall that the magnetic force has been expanded into

$$F_y^{\rm mag}(y_1,\bar{y}_1) = \left.\frac{dF_y^{\rm mag}}{dy_1}\right|_{\bar{y}_1=0} y_1 + \left.\frac{dF_y^{\rm mag}}{d\bar{y}_1}\right|_{y_1=0} \bar{y}_1 . \tag{2.39}$$

The ac field comes from the betatron oscillation of the whole beam and has its source from the second term on the right side only. We know that, for non-penetrating fields, the first term gives rise to the incoherent electric image coefficient ϵ_1^V multiplied by $-\beta^2$. We also know that when we replace y_1 by $\bar{y}_1$, the two terms together gives rise to $-\beta^2$ times the coherent electric image coefficient ξ_1^V, which is always non-penetrating. Therefore, the ac magnetic image from the betatron oscillation of the beam contributes $-\beta^2(\xi_1^V - \epsilon_1^V)$ which is the last term of Eq. (2.38). As for the first term on the right side of Eq. (2.39), it describes a witness particle oscillating transversely inside a stationary beam. This particle and its images contribute dc magnetic fields that penetrate the vacuum chamber and landing at the magnet poles. Its contribution is therefore ϵ_2^V, which is the second last term of Eq. (2.38). After re-arrangement, the coherent tune shift with penetrating fields read

$$\Delta\nu_{\rm coh}^{V,H} = -\frac{Nr_0R}{\pi\gamma\beta^2\nu_0^{V,H}}\left[\frac{(1-\beta^2)\xi_1^{V,H}}{h^2} + \beta^2\frac{\epsilon_1^{V,H}}{h^2} + \mathcal{F}\beta^2\frac{\epsilon_2^{V,H}}{g^2}\right] . \tag{2.40}$$

2.6 BUNCHED BEAMS

For bunched beam, we would like to compute the maximum tune shifts when the beam current is at its local maximum. We therefore divide by the bunching factor B suitably so that the bunch intensity will be properly enhanced. Notice that ac magnetic field now comes from two sources: transverse betatron oscillation of the bunch and longitudinal or axial bunching of the bunch. Although both effects are ac, their frequencies are in general very different. The frequency of transverse betatron oscillation is $(n-\nu_0^{V,H})\omega_0/(2\pi)$, where n is the revolution harmonic closest to the tune. These frequencies are therefore only

fractions of the revolution frequency. On the other hand, the axial bunch frequency is a $h\omega_0/(2\pi)$ with h the rf harmonic, which is many times revolution frequency. For this reason, we consider the ac magnetic fields arriving from axial bunching *always non-penetrating*, while the ac magnetic fields arriving from betatron oscillation sometimes non-penetrating and sometimes penetrating.

In the expressions below, we try also to include the effect of trapped particles that carry charges of opposite sign. Take a proton beam, for example, electrons can be trapped, giving a neutralization coefficient χ_e, which is defined as the ratio of the total number of trapped electrons to the total number of protons. (For antiproton beam, the particles trapped are positively charged ions.) The trapped electrons will not travel longitudinally. Therefore, they only affect the electric force but not the magnetic force. In other words, for electric contributions, we replace 1 by $(1-\chi_e)$.

The incoherent tune shift for a bunched beam is expressed as

$$\Delta\nu_{\rm incoh}^{V,H}=-\frac{Nr_0R}{\pi\gamma\beta^2\nu_0^{V,H}}\left[\frac{1-\chi_e}{B}\frac{\epsilon_1^{V,H}}{h^2}+\mathcal{F}\beta^2\frac{\epsilon_2^{V,H}}{g^2}-\beta^2\left(\frac{1}{B}-1\right)\frac{\epsilon_1^{V,H}}{h^2}+(1-\chi_e-\beta^2)\frac{\epsilon_{\rm spch}^{V,H}}{a_V^2}\right]. \tag{2.41}$$

↑ electric image in vacuum chamber; ↑ magnetic image in magnet poles; ↑ ac magnetic image from axial bunching; ↑ self-field

The second term represents magnetic fields of a stationary beam and its images and therefore the usual incoherent magnetic image coefficient $\epsilon_2^{V,H}$, which describes dc magnetic fields penetrating the vacuum chamber and land at the magnet poles. Here, there is no division by the bunching factor B, because we are talking about the dc fields coming from the *average* beam current.

The third term is for the ac magnetic fields generated from axial bunching and a division by B is therefore necessary. Since the ac magnetic fields are non-penetrating, their contribution is the same as that of the incoherent electric field and therefore the factor $-\beta^2\epsilon_1^{V,H}$. We must remember that there is a dc part which we have considered already and must not be included here again. For this reason, we need to replace B^{-1} by $B^{-1}-1$. After re-arrangement, this incoherent tune shift can be rewritten as

$$\Delta\nu_{\rm incoh}^{V,H}=-\frac{Nr_0R}{\pi\gamma\beta^2\nu_0^{V,H}}\left[\left(\frac{1-\chi_e-\beta^2}{B}+\beta^2\right)\frac{\epsilon_1^{V,H}}{h^2}+\mathcal{F}\beta^2\frac{\epsilon_2^{V,H}}{g^2}+(1-\chi_e-\beta^2)\frac{\epsilon_{\rm spch}^{V,H}}{a_V^2}\right]. \tag{2.42}$$

For coherent motion with penetrating magnetic fields from betatron oscillation, we

have

$$\Delta\nu_{\rm coh}^{V,H} = -\frac{Nr_0R}{\pi\gamma\beta^2\nu_0^{V,H}}\left[\frac{1-\chi_e}{B}\frac{\xi_1^{V,H}}{h^2} + \mathcal{F}\beta^2\frac{\xi_2^{V,H}}{g^2} - \beta^2\left(\frac{1}{B}-1\right)\frac{\xi_1^{V,H}}{h^2}\right] . \tag{2.43}$$

↑ electric image in vacuum chamber; ↑ magnetic image in magnet poles; ↑ ac magnetic image from axial bunching

The magnetic fields divide into the dc part and the ac part in exactly the same way as Eq. (2.41), the expression for incoherent tune shift. Because we are talking about coherent tune shifts, the coefficients $\epsilon_2^{V,H}$ and $\epsilon_1^{V,H}$ are replaced, respectively by $\xi_2^{V,H}$ and $\xi_1^{V,H}$. After re-arrangement, the coherent tune shifts with penetrating magnetic fields from betatron oscillation can be rewritten as

$$\Delta\nu_{\rm coh}^{V,H} = -\frac{Nr_0R}{\pi\gamma\beta^2\nu_0^{V,H}}\left[\left(\frac{1-\chi_e-\beta^2}{B}+\beta^2\right)\frac{\xi_1^{V,H}}{h^2} + \mathcal{F}\beta^2\frac{\xi_2^{V,H}}{g^2}\right] . \tag{2.44}$$

Finally, we come to ac magnetic fields that are non-penetrating coming from both axial bunching and betatron oscillation. The coherent tune shifts are

$$\Delta\nu_{\rm coh}^{V,H} = -\frac{Nr_0R}{\pi\gamma\beta^2\nu_0^{V,H}}\left[\frac{1-\chi_e}{B}\frac{\xi_1^{V,H}}{h^2} + \mathcal{F}\beta^2\frac{\epsilon_2^{V,H}}{g^2} - \beta^2\frac{\xi_1^{V,H}-\epsilon_1^{V,H}}{h^2} - \beta^2\left(\frac{1}{B}-1\right)\frac{\xi_1^{V,H}}{h^2}\right] . \tag{2.45}$$

↑ electric image in vacuum chamber; ↑ magnetic image in magnet poles; ↑ ac magnetic image from transverse motion; ↑ ac magnetic image from axial bunching

Here, the axial bunching parts are very exactly the same as in Eq. (2.43) because they describe exactly the same ac magnetic fields coming from axial bunching. As for the dc magnetic fields, the contribution in Eq. (2.43) come from both terms of Eq. (2.39) and contribute the coefficient $\xi_2^{V,H}$. Here the dc magnetic fields come from only the first term of Eq. (2.39) and contribute $\epsilon_1^{V,H}$ instead, for exactly the same reason as in Eq. (2.36). The part of the second term of Eq. (2.39) that comes from betatron oscillation of the beam gives rise to the second last term of Eq. (2.45), for exactly the same reason as in Eq. (2.36). After re-arrangement, this coherent tune shift takes the form

$$\Delta\nu_{\rm coh}^{V,H} = -\frac{Nr_0R}{\pi\gamma\beta^2\nu_0^{V,H}}\left[\frac{1-\chi_2-\beta^2}{B}\frac{\xi_1^{V,H}}{h^2} + \mathcal{F}\beta^2\frac{\epsilon_1^{V,H}}{g^2} + \beta^2\frac{\epsilon_2^{V,H}}{g^2}\right] . \tag{2.46}$$

2.7 OTHER VACUUM CHAMBER GEOMETRIES

The electric and magnetic image coefficients have been computed for other geometries of the vacuum chamber: circular cross section, rectangular cross section, and elliptical cross section, and even with the beam off-center [2, 3]. The computation for the rectangular and elliptical cross sections involve one or more than one conformal mappings and the results are given in terms of elliptical functions.

The situation of circular cross section with an on-center beam is rather simple. Consider a line charge of linear density λ_1 at location $x = 0$ and $y = \bar{y}_1$ inside the cylindric beam pipe of radius b with infinitely conducting walls. We place an image line charge of linear density λ_2 at location $x = 0$ and $y = \bar{y}_2$ as shown in left plot of Fig. 2.4.

The electric potential at point P on a chamber wall at an angle θ is given by

$$V_P = -\frac{e\lambda_1}{2\pi\epsilon_0}\ln r_1 + \frac{e\lambda_2}{2\pi\epsilon_0}\ln r_2 \ , \tag{2.47}$$

where

$$\begin{cases} r_1^2 = \bar{y}_1^2 + b^2 - 2\bar{y}_1 b\cos\theta \ , \\ r_2^2 = \bar{y}_2^2 + b^2 - 2\bar{y}_2 b\cos\theta \ . \end{cases} \tag{2.48}$$

Notice that if we assert that

$$\bar{y}_2 = \frac{b^2}{\bar{y}_1} \qquad \text{and} \qquad \lambda_2 = -\lambda_1 \ , \tag{2.49}$$

we obtain from the first assertion that $r_2^2 = r_1^2(b^2/\bar{y}_1^2)$. Then the second assertion ensures that the electric potential V_P vanishes aside from a constant for any point on the wall of the cylindrical vacuum chamber.

To compute the image force, place a witness line charge at $x = x_1$ and $y = y_1$, illustrated in the right plot of Fig. 2.4. Then the electric force exerted on the witness charge by the image has y component

$$\frac{F_y^{\text{elec}}}{e} = -\frac{e\lambda_1}{2\pi\epsilon_0}\frac{\dfrac{b^2}{\bar{y}_1} - y_1}{x_1^2 + \left(\dfrac{b^2}{\bar{y}_1} - y_1\right)^2} \longrightarrow -\frac{e\lambda_1}{2\pi\epsilon_0}\frac{\bar{y}_1}{b^2} \ , \tag{2.50}$$

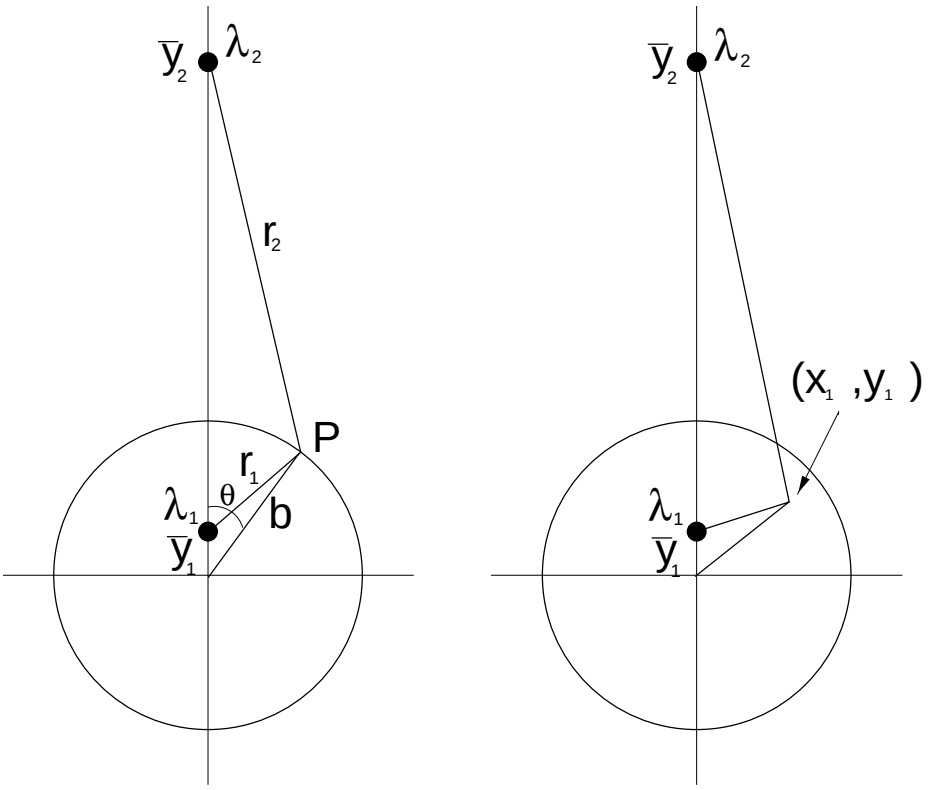

Figure 2.4: Left plot illustrates a line charge density λ_1 inside a cylindrical beam pipe offset vertically by $\bar{y}_1$. There is an image line charge density λ_2 at $\bar{y}_2$ such that the electric potential vanishes at every point P at the beam pipe. Right plot shows the combined electric force acting on a witness line charge at (x_1, y_1).

where in the last step only terms linear in y_1 and $\bar{y}_1$ are retained. According to Eq. (2.13),

$$\Delta\nu^V_{\rm incoh} = -\frac{Nr_0R}{\pi\gamma\beta^2\nu_0^V}\,\frac{\epsilon_1^V}{b^2} \qquad \text{and} \qquad \Delta\nu^V_{\rm coh} = -\frac{Nr_0R}{\pi\gamma\beta^2\nu_0^V}\,\frac{\xi_1^V}{b^2}\ , \tag{2.51}$$

we immediately obtain the incoherent and coherent electric image coefficients for a circular beam pipe:

$$\epsilon_1^V = 0 \qquad \text{and} \qquad \xi_1^V = \frac{1}{2}\ . \tag{2.52}$$

Because of the cylindrical symmetry, we also have

$$\epsilon_1^H = 0 \qquad \text{and} \qquad \xi_1^H = \frac{1}{2}\ . \tag{2.53}$$

It is not surprising to see the incoherent electric image coefficients vanish. This is because at the point of observation of the witness charge, $\vec{\nabla}\cdot\vec{E} = 0$, leading to $\epsilon_1^V + \epsilon_1^H = 0$.

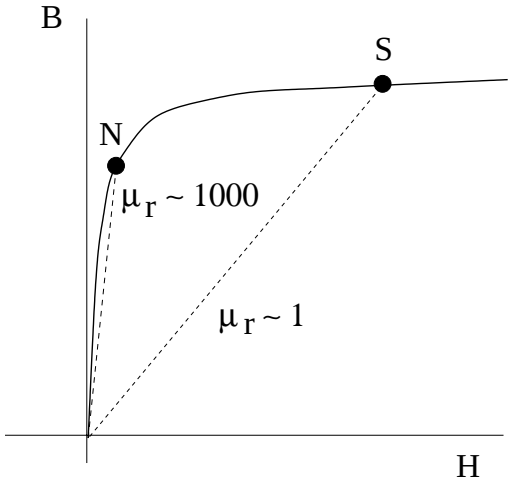

Figure 2.5: B-H hysteresis plot showing the operation of normal temperature magnet at Point N where the relative magnetic permeability μ_r is large. The operation of superconducting magnet is at Point S where the iron yoke is at saturation and $\mu_r \approx 1$.

Mathematically, it is impossible to compute the magnetic image coefficients for a closed cylindrical iron yoke that has infinite relative permeability. In fact, no solution exists for a closed iron yoke of any geometry. This is because of Ampere's law,

$$\oint \vec{H} \cdot d\vec{\ell} = I \ . \tag{2.54}$$

For a beam of current I, the component of magnetic field $\vec{H}$ along the inner surface if the iron yoke is therefore nonzero. Thus, the magnetic flux density $\vec{B}$ inside the yoke becomes infinite. Speaking in the reverse order, if the magnetic flux density inside the yoke is finite, the magnetic field $\vec{H}$ along the inner surface must vanish. From Ampere's law, $I = 0$, or no current is allowed to flow through the yoke.

For a normal temperature magnet, we like to operate in the linear region of the B-H hysteresis curve, for example Point N in Fig. 2.5, in order to take advantage of the large relative magnetic permeability, $\mu_r \sim 1000$. Then, most of the magnetic flux density across the pole gap is supplied by μ_r and only a few percents come from the winding current. Such operation limits the magnetic flux density to $B_{\max} \sim 1.8$ T. This explains why the iron yoke is mostly made up of two pieces glued together with some medium. In that case, $\vec{H}$ will only be large in the medium but relatively small inside the yoke and a much larger beam current will be allowed.

The story for superconducting magnets is quite different. Here, the magnetic flux density is mostly supplied by the high winding current, while the iron yoke is always saturated. The operation point in the hysteresis curve is now at S of Fig. 2.5 in the large H region where the local slope is 1. Thus the relative permeability μ_r becomes close to 1 and is very much less than the linear region of the curve. If the same closed iron yoke is used, the maximum beam current allowed by Ampere's law becomes ~ 1000 times larger.

When the relative permeability is finite, the Laplace equation can still be solved using the image method, provided there is sufficient symmetry in the geometry. Readers with interest are referred to, for example, the book by Binns and Lawrenson [4].

In Table 2.1, we tabulate the self-field coefficients for uniformly charged beams and image coefficients for centroid beams [5].

2.8 INCOHERENCE VERSUS COHERENCE

Usually, people say that a large incoherent space-charge tune spread will encompass a lot of parametric resonances and lead to instability. The common rule of thumb is that incoherent self-field tune spread should not exceed ~ 0.40. However, this self-field tune spread at injection has never been a well-measured beam parameter. It is difficult to measure because low-energy rings are usually ramped very rapidly. Thus, the self-field tune spread diminishes very quickly as the energy of the beam increases. Most low-energy rings that have large space-charge tune spread are ramped by a resonator. To measure the self-field tune spread, we must disconnect the magnet winding currents from the resonator so as to provide a longer interval for which the beam energy does not change. This is not always possible, because the beam will generally become unstable if it is allowed to stay at such low energy for a long time. If the condition is available, however, the tune spread can be measured by a technique called rf knockout. A narrow band rf signal is used to excite the beam. Those particles with the correct tune resonate with the driving signal and are lost. Since only a small fraction of the beam resonates, this resonating frequency of rf signal corresponds to the incoherent tune of the beam. Another way is to perform a Schottky scan which shows the tunes of individual particles. The coherent tune shifts can be measured by the same rf knockout method. If the exciting rf signal hits a coherent tune, the whole beam will be lost.

Machida and Ikegami [6] pointed out at the space-charge workshop at Shelter Island

Table 2.1: Self coefficients for uniformly charged beam and image coefficients for centered beam.

Coeff.	Circular	Elliptical	Parallel Plates	Comments
ϵ^V_{spch}	$\frac{1}{2}$	$\frac{a_V}{a_H + a_V}$		Combined electric and magnetic self-field
ϵ^H_{spch}	$\frac{1}{2}$	$\frac{a_V^2}{a_H(a_H + a_V)}$		
ϵ^V_1	0	$\frac{h^2}{12w^2}\left[(1+k'^2)\left(\frac{2K}{\pi}\right)^2 - 2\right]$	$\frac{\pi^2}{48}$	Electric field and ac magnetic field with ξ_1
ϵ^H_1	0	$\frac{-h^2}{12w^2}\left[(1+k'^2)\left(\frac{2K}{\pi}\right)^2 - 2\right]$	$\frac{-\pi^2}{48}$	
ϵ^V_2	*	*	$\frac{\pi^2}{24}$	Magnetic field
ϵ^H_2	*	*	$\frac{-\pi^2}{24}$	
ξ^V_1	$\frac{1}{2}$	$\frac{h^2}{4w^2}\left[\left(\frac{2K}{\pi}\right)^2 - 1\right]$	$\frac{\pi^2}{16}$	Electric field and ac magnetic field with ϵ_1
ξ^H_1	$\frac{1}{2}$	$\frac{h^2}{4w^2}\left[1 - \left(\frac{2K}{\pi}\right)^2\right]$	0	
ξ^V_2	*	*	$\frac{\pi^2}{16}$	Magnetic field
ξ^H_2	*	*	0	

* ϵ_2 and ξ_2 for closed magnetic boundary (e.g., circular or elliptic) cannot be calculated for $\mu \to \infty$, since the induced magnetic field would not permit a charged beam to pass through. Closed magnetic yokes are used in superconducting magnets, but there the coefficients $\epsilon_2 = \xi_2 \to 0$, since the magnetic material is driven completely into saturation ($\mu \to 1$).

$K(k)$ is the complete elliptic integral of the first kind. k is determined from $(w-h)/(w+h) = \exp(-\pi k'/k)$ where w and h are the horizontal and vertical axes (not radii) of the elliptical cross section, $d = \sqrt{w^2 - h^2}$, and $K' = K(k')$ with $k' = \sqrt{1-k^2}$.

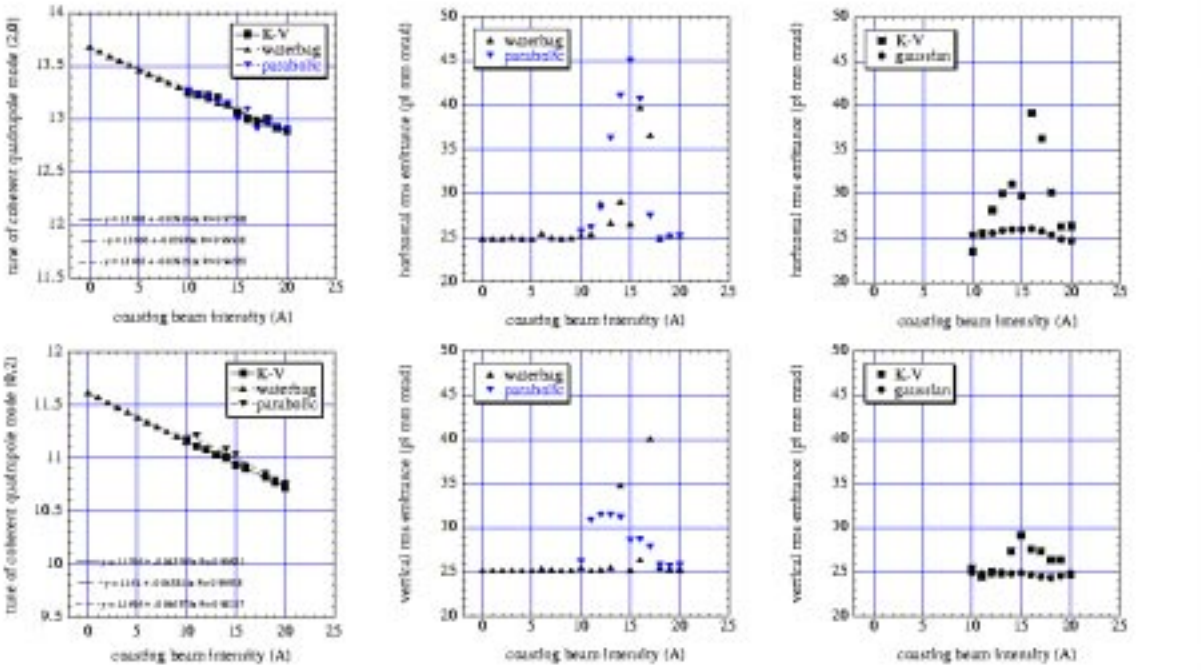

Figure 2.6: (color) Tune of coherent quadrupole mode (left) and rms emittance at 512 turns after injection (center and right) versus beam intensity. Upper figures show horizontal results and lower ones vertical. Rms emittance growth is observed when either the horizontal or vertical coherent quadrupole tune becomes integer. (Reproduced from Ref. [6]).

that it is the *coherent* rather than the *incoherent* tune shifts that determine the instability of a beam. In fact, this is quite reasonable. When the bunch is oscillating at an integer coherent tune, we have the usual integer resonance. This leads to an instability because all particles are performing betatron oscillations with a tune component that is at an integer. The whole beam will become unstable. On the other hand, if the incoherent tune spread covers an integer resonance, only *a small amount* of particles are hitting the integer resonance; thus the whole beam may not be unstable. The coherent betatron tune is not affected by space charge when the image forces are small. This is because the centroid of the bunch does not see any space-charge force. On the other hand, the coherent quadrupole betatron tune and coherent sextupole betatron tune will be affected by space charge. Therefore, when they hit a resonance, there will be instability. This is demonstrated by the simulation of Machida and Ikegami in Fig. 2.6. In the simulation, the horizontal coherent quadrupole tune hits the integer of 13 when the beam intensity

reaches $\sim$ 15 A. We do see that the horizontal emittance increases rapidly around the beam intensity of 15 A. The vertical coherent quadrupole tune hits the integer 11 when the beam intensity is raised to around 13 to 15 A. The vertical emittance increases also around those intensities. However, we do not see any growth of emittance when the coherent quadrupole tunes cross half integers.

2.9 CONNECTION WITH IMPEDANCE

In Eq. (2.5), the term proportional to y on the right side is absorbed into the betatron tune shift so that ν_0^V becomes ν_V. The equation becomes

$$\frac{d^2y}{ds^2} + \frac{(\nu^V)^2}{R^2}y = \frac{1}{\gamma m v^2}\left.\frac{\partial\langle F_{\rm beam}(y,\bar{y})\rangle}{\partial\bar{y}}\right|_{y=0}\bar{y}\ . \tag{2.55}$$

The coherent force on the right is related to the transverse wake function and therefore the transverse impedance. The connection can be easily made using Eq. (1.24), which says

$$\left.\frac{\partial\langle F_{\rm beam}(y,\bar{y})\rangle}{\partial\bar{y}}\right|_{y=0}\bar{y} = \frac{ieZ_1^\perp\beta I\bar{y}}{C} = \frac{ie^2Z_1^\perp\beta^2 c\bar{y}}{C}\ . \tag{2.56}$$

On the other hand, in Eq. (2.12), according to the the definition of the image coefficient,

$$eE^V(y,\bar{y})|_{y=0} = \frac{e^2\lambda Z_0 c}{\pi}\frac{\xi_1^V-\epsilon_1^V}{h^2}\bar{y}\ . \tag{2.57}$$

As a result, we obtain

$$Z_1^\perp = -i\frac{Z_0C}{\pi\gamma^2\beta^2}\frac{\xi_1^V-\epsilon_1^V}{h^2}\ . \tag{2.58}$$

For a circular beam pipe, $\xi_1^V = \frac{1}{2}$ and $\epsilon_1^V = 0$. This is just exactly the second half of the transverse space-charge impedance in Eq. (1.32). Thus, the transverse space-charge impedance can be interpreted as the summation of two parts: the part proportional to a^{-2} is the self-field contribution and the part proportional to b^{-2} is the wall image contribution. We can therefore rewrite the expression in a more general way as

$$Z_1^{V,H} = i\frac{Z_0C}{\pi\gamma^2\beta^2}\left[\frac{\epsilon_{\rm spch}^{V,H}}{a_V^2} - \frac{\xi_1^{V,H}-\epsilon_1^{V,H}}{h^2}\right]\ , \tag{2.59}$$

where h is the half height of the vacuum chamber.

It is important to distinguish the difference between the force generating the coherent tune shift and the force generating the transverse impedance. The former involves the ξ_1 coefficient while the later involves $\xi_1 - \epsilon_1$. The coherent tune shift is the result of all forces acting on the center of the beam $\bar{y}$, while the transverse impedance comes from the force generated by the center motion of the beam on an individual particle. In other words,

$$\Delta\nu \propto \left.\frac{\partial\langle F_{\rm beam}(y,\bar{y})\rangle}{\partial y}\right|_{\bar{y}=0} + \left.\frac{\partial\langle F_{\rm beam}(y,\bar{y})\rangle}{\partial \bar{y}}\right|_{y=0} ,$$

$$Z_1^\perp \propto \left.\frac{\partial\langle F_{\rm beam}(y,\bar{y})\rangle}{\partial \bar{y}}\right|_{y=0} . \tag{2.60}$$

Thus, the results can be very different. Take the example of a beam between two infinite conducting planes. Because of horizontal translational invariance, the horizontal force acting at the center of the beam vanishes independent of whether the beam is moving horizontally or vertically. The horizontal coherent tune shift therefore vanishes. However, the horizontal motion of the center of mass of the beam does provide a horizontal force on an individual particle, which may not be moving with the center of mass. That individual particle will therefore see a nonvanishing transverse impedance.

2.10 MORE ABOUT WAKE FUNCTIONS

Most the time the vacuum chamber is not cylindrical in shape. Thus, the expansion into circular harmonics in Sec. 1.4 cannot be performed. Here, we want to emphasize that it is always completely valid to expand $\vec{E}$ and $\vec{B}$ into circular harmonics. However, when the boundary conditions are applied, $\vec{E}$ and $\vec{B}$ of different circular harmonics will be mixed together, and so are the wake functions W_m for different m's. In other words, equations corresponding to an individual m are not independent, thus rendering the expansion useless. For this reason, we need to give slightly different definitions for the wake functions when there is no cylindrical symmetry.

Consider a test particle carrying charge q_1 traveling with velocity v longitudinally along a designated path in a vacuum chamber. A witness particle of charge q_2 at a distance z behind along the same path sees a longitudinal force $F_0^\parallel$ and a transverse force $F_0^\perp$ due to the wake fields of the test particle. In general, these forces depend also on the location s of the test particle along the beam pipe. However, when we apply the impulse approximation, these forces are integrated over s for a long length ℓ of the beam pipe

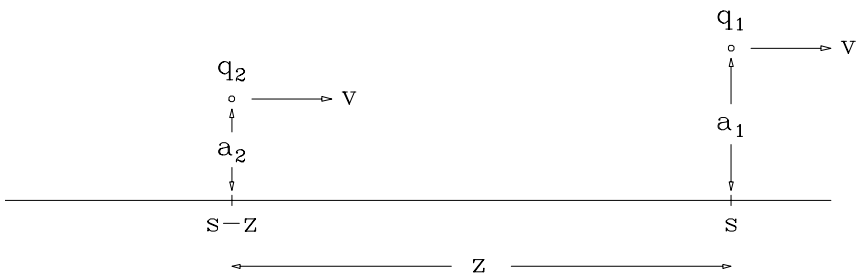

Figure 2.7: Test particle with charge q_1 at an offset of a_1 from the designated path leaves wake fields to the witness particle with charge q_2 at an offset of a_2 at a distance z behind.

and become functions of z only. For a circular machine, ℓ is taken as the circumference C. Unlike the situation of traveling along the symmetry axis of a cylindrical beam pipe, here there is always an average transverse force $\langle F_0^\perp \rangle$. This transverse force comes mostly from the images in the walls of the vacuum chamber. It should be weak in general and can therefore be incorporated into the betatron tunes as tune shifts in the way discussed above in Sec. 2.1.

The *longitudinal wake function* is defined as

$$W_0'(z) = -\frac{\langle F_0^\parallel \rangle \ell}{q_1 q_2} \ , \tag{2.61}$$

where $\langle F_0^\parallel \rangle \ell$ denotes the longitudinal integrated wake force or impulse.

If the path of the source particle is displaced transversely by a_1 from the designated path as in Fig. 2.7, the witness particle displaced by a_2 at a distance z behind will see a longitudinal force $F_1^\parallel$ and a transverse force $F_1^\perp$. The *transverse wake function* is now defined by

$$W_1(z) = -\lim_{a_1, a_2 \to 0} \frac{(\langle F_1^\perp \rangle - \langle F_0^\perp \rangle)\ell}{a_1 q_1 q_2} \ , \tag{2.62}$$

where the transverse force along the designated path $\langle F_0^\perp \rangle$ has been subtracted away because it has been taken care of already as tune shifts. Defined in this way, $W_0'(z)$ and $W_1(z)$ will be the same as the $m = 0$ longitudinal wake function and the $m = 1$ transverse wake function defined in Chapter 1.

2.11 EXERCISES

2.1. Consider a beam with bi-parabolic or semi-circular distribution

$$\rho(r) = \frac{2e\lambda}{\pi\hat{r}^2}\left(1 - \frac{r^2}{\hat{r}^2}\right) , \tag{2.63}$$

where $\hat{r}$ is the radial extent of the beam and λ is the linear particle density.
(1) Compute the self-field or space-charge incoherent tune shift at the center of the beam where it is maximal and show that the space-charge coefficient defined in Eq. (2.25) is $\epsilon_{\rm spch} = 1$.
(2) Explain how one can understand that $\epsilon_{\rm spch}$ for this distribution is in between $\epsilon_{\rm spch} = \frac{1}{2}$ for uniform distribution and $\epsilon_{\rm spch} \approx \frac{3}{2}$ for bi-Gaussian distribution.

2.2. Consider a beam with elliptic cross section and uniform particle distribution.
(1) Show that the electric potential

$$V(x,y) = -\frac{e\lambda}{2\pi\epsilon_0}\frac{1}{a_H + a_V}\left(\frac{x^2}{a_H} + \frac{y^2}{a_V}\right) \tag{2.64}$$

for $x^2/a_H^2 + y^2/a_V^2 < 1$ and 0 otherwise, satisfies the Laplace equation

$$\nabla^2 V(x,y) = -\frac{e\lambda}{\pi\epsilon_0 a_H a_V} , \tag{2.65}$$

where λ is the linear particle density of the beam.
(2) Show that inside the beam, the transverse electric fields are

$$E_x = \frac{e\lambda}{\pi\epsilon_0}\frac{x}{a_H(a_H + a_V)}$$

$$E_x = \frac{e\lambda}{\pi\epsilon_0}\frac{y}{a_V(a_H + a_V)} \tag{2.66}$$

(3) Comparing with the electric field components inside a cylindrically symmetric beam of radius a, show that the space-charge tune shift coefficients, defined in Eq. (2.25), inside this beam of elliptic cross section are

$$\epsilon_{\rm spch}^H = \frac{a_V^2}{a_H(a_H + a_V)} \qquad \text{and} \qquad \epsilon_{\rm spch}^V = \frac{a_V}{a_H + a_V} . \tag{2.67}$$

2.3. We are going to derive the electric potential $V(x,y,z)$ for a 3-dimensional charge distribution,

$$\rho(x,y,z) = \frac{eN}{(2\pi)^{3/2}\sigma_x\sigma_y\sigma_z}\exp\left[-\frac{x^2}{2\sigma_x^2}-\frac{y^2}{2\sigma_y^2}-\frac{z^2}{2\sigma_z^2}\right] , \tag{2.68}$$

following the method of Takayama [7], where N is the total number of particles.
(1) Show that the Green function of the Laplace equation can be written as

$$G(\vec{r},\vec{\xi}) = \frac{1}{4\pi|\vec{r}-\vec{\xi}|} = \frac{1}{2\pi^{3/2}}\int_0^\infty dq\, e^{-|\vec{r}-\vec{\xi}|^2q^2} . \tag{2.69}$$

In other words, $G(\vec{r},\vec{\xi})$ satisfies

$$\nabla^2 G(\vec{r},\vec{\xi}) = -\delta(\vec{r}-\vec{\xi}) . \tag{2.70}$$

(2) Changing the variable of integration to $t = q^{-2}$, show that the electric potential can be written as

$$V(x,y,z) = \frac{1}{4\pi^{3/2}\epsilon_0}\int_0^\infty \frac{dt}{t^{3/2}}\int_{-\infty}^\infty d\vec{\xi}\,\rho(\vec{\xi})e^{-|\vec{r}-\vec{\xi}|^2/t} . \tag{2.71}$$

(3) With ρ given by Eq. (2.68), derive the electric potential

$$V(x,y,z) = \frac{eN}{4\pi^{3/2}\epsilon_0}\int_0^\infty dt\,\frac{\exp\left[-\frac{x^2}{(2\sigma_x^2+t)}-\frac{y^2}{(2\sigma_y^2+t)}-\frac{z^2}{(2\sigma_z^2+t)}\right]}{\sqrt{(2\sigma_x^2+t)(2\sigma_y^2+t)(2\sigma_z^2+t)}} . \tag{2.72}$$

2.4. Consider a beam with bi-Gaussian transverse charge distribution,

$$\rho(x,y) = \frac{e\lambda}{2\pi\sigma_x\sigma_y}\exp\left(-\frac{x^2}{2\sigma_x^2}-\frac{y^2}{2\sigma_y^2}\right) , \tag{2.73}$$

where σ_x and σ_y are the rms width and height, and λ is the linear particle density.
(1) From Eq. (2.72), show that the electric potential is

$$V(x,y) = \frac{e\lambda}{4\pi\epsilon_0}\int_0^\infty dt\,\frac{\exp\left[-\frac{x^2}{(2\sigma_x^2+t)}-\frac{y^2}{(2\sigma_y^2+t)}\right]}{\sqrt{(2\sigma_x^2+t)(2\sigma_y^2+t)}} . \tag{2.74}$$

(2) Show that the transverse electric fields are

$$E_x = \frac{e\lambda x}{4\pi\epsilon_0}\int_0^\infty dt\,\frac{\exp\left[-\frac{x^2}{(2\sigma_x^2+t)}-\frac{y^2}{(2\sigma_y^2+t)}\right]}{(2\sigma_x^2+t)\sqrt{(2\sigma_x^2+t)(2\sigma_y^2+t)}} ,$$

$$E_y \to E_x \quad \text{with} \;\; x \to y, \quad y \to x \; . \tag{2.75}$$

(3) The self-field or space-charge tune shifts are at their maxima at the center of the beam, or $x \to 0$ and $y \to 0$. Show that they are given by Eq (2.32) with

$$\begin{aligned} \sigma^2 &\to \frac{\sigma_x(\sigma_x + \sigma_y)}{2} \quad \text{for } \Delta\nu^H_{\text{spch incoh}} \\ \sigma^2 &\to \frac{\sigma_y(\sigma_x + \sigma_y)}{2} \quad \text{for } \Delta\nu^V_{\text{spch incoh}} \; . \end{aligned} \tag{2.76}$$

Bibliography

[1] L.J. Laslett, Proceedings of 1963 summer Study on Storage Rings, BNL-Report 7534, p. 324; L.J. Laslett and L. Resegotti, Proceedings of VIth Int. Conf. on High Energy Accelerators, Cambridge, MA, 1967, p. 150.

[2] B. Zotter, CERN ISR-TH/72-8 (1972); CERN ISR-TH/74-11 (1974); CERN IST-TH/74-38 (1974); CERN ISR-TH/75-17 (1975); Proceedings of VIth National particle Accelerator Conf., Washington DC, 1974 (IEEE, 1975).

[3] K.Y. Ng, Particle Accelerators **16**, 63 (1984).

[4] K.J. Binns and P.J. Lawrenson, *Analysis and Computation of Electric and Magnetic Field Problems*, 2nd Ed., Pergamon Press, 1973.

[5] G. Guignard, CERN 77-10 (1977).

[6] Machida, S., and Ikegami, M,, *Proceedings of Workshop on Space Charge Physics in High Intensity Hadron Rings*, p.73, Ed. Luccio, A.U., and Weng, W.T., (Shelter Island, New York, May 4-7, 1998).

[7] K. Takayama, Lett. Al Nuovo Cimento **34**, 190 (1982).